Weakly Nonlinear Analysis of a Localized Disturbance in Poiseuille Flow

By D. Ponziani, C. M. Casciola, F. Zirilli, and R. Piva

In this article, we investigate, via a perturbation analysis, some important nonlinear features related to the process of transition to turbulence in a wall-bounded flow subject to a spatially localized disturbance that is harmonic in time. We show that the perturbation expansion, truncated at second order, is able to capture the generation of streamwise vorticity as a weakly nonlinear effect. The results of the perturbation approach are discussed in comparison with direct numerical simulation data for a sample case by extracting the contribution of the different orders. The main aim is to provide a tool to select the most effective nonlinear interactions to enlighten the essential features of the transitional process.

1. Introduction

Transition to turbulence in a wall-bounded flow has long been studied, but some fundamental aspects still need further investigation. If we consider only small amplitude disturbances, we can linearize the Navier–Stokes equations about a given laminar solution (base flow) to obtain the Orr–Sommerfeld, Squire system. The associated eigenvalue problem determines the critical value of the control parameter; namely, the Reynolds number. Above the

Address for correspondence: Dr. D. Ponziani, Dipartimento di Meccanica e Aeronautica, Universitá di Roma *La Sapienza* via Eudossiana 18, 00184 Roma, Italy.

STUDIES IN APPLIED MATHEMATICS 105:121–141
© 2000 by the Massachusetts Institute of Technology
Published by Blackwell Publishers, 350 Main Street, Malden, MA 02148, USA, and 108 Cowley Road, Oxford, OX4 1JF, UK.

critical Reynolds number, the flow is linearly unstable (at least one eigenvalue with positive real part exists) and arbitrarily small perturbations initiate a process that eventually leads to turbulence (see Drazin and Reid [1]).

As a characteristic feature of wall-bounded shear flows, transition can also occur for Reynolds numbers less than the critical value. In this subcritical regime, the base flow is linearly stable, and the effects of the nonlinear terms of the Navier–Stokes equations are crucial to explain the transition process. Nevertheless, the basic mechanism that is able to amplify the initial perturbation is essentially linear, as discussed in a number of contributions (see Stuart [2], Ellingsen and Palm [3], and Landahl [4]). Actually the Orr–Sommerfeld, Squire system, which defines a linear operator that is non-normal in the energy norm (i.e., the L^2 norm of the perturbation velocity field) originates a substantial increase of the perturbation amplitude (see Trefethen et al. [5] and Reddy et al. [6]).

In the context of linearized analysis, after a phase of transient growth, the perturbation is bound to decay, because the flow is asymptotically stable. By retaining the nonlinear terms of Navier–Stokes equations instead, the growth of the perturbation during the transient may be sufficiently large to provide the loss of stability of the base flow. In fact, the nonlinear evolution is characterized by a threshold effect such that, for fixed Re, only sufficiently large disturbances are able to produce transition.

There is evidence that turbulence breakdown, in subcritical transition, is associated with the formation of a system of low- and high-speed streaks that are related to the presence of streamwise vortices. Because particles near the wall and in the bulk region carry low and high momentum, respectively, the vortices, by advecting them from the walls toward the bulk of the flow and vice versa, are responsible for the formation of low- and high-speed regions. This phenomenon, known as lift-up effect [4], also may be described in terms of a linear analysis (see Butler and Farrel [7]), provided suitable initial conditions, which imply the presence of streamwise vorticity, are imposed. However, there are reasons to believe that the nonlinear interactions are prevailing in the process of generation of streaks and vortex regeneration. The first step of the sequence of these events has been successfully investigated by Reddy et al. in [8] and by Schmid and Henningson in [9] considering the transition initiated by optimal streamwise vortices and by a pair of oblique Tollmien–Schlicting waves, respectively. Here, we also study the streaks formation, but starting with a more general disturbance in the framework of nonlinear dynamics. In such a case, the direct numerical simulation (DNS) and the experimental analysis, which are mostly used to capture these nonlinear aspects, do not provide, beyond the actual evidence, the tools to disentangle the above mentioned sequence of physical events. To solve this, we introduce a theoretical model able to analyze the early nonlinear stages of the transition process by a weakly nonlinear approach based on a pertur-

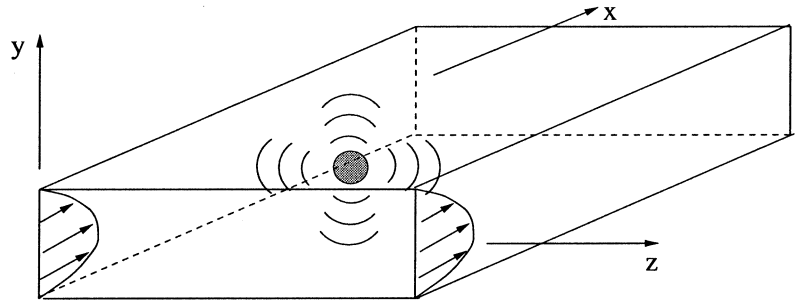

Figure 1. The physical sketch for the sample problem.

bative method. The basic solution technique for the issuing linear problems is essentially based on expansion in terms of the Orr–Sommerfeld, Squire eigenfunctions, see Henningson and Schmid [10], Gaster [11], although in principle, a direct time-stepping procedure could also have been employed (see Criminale et al. [12]). We consider here a channel flow where low- and high-speed streaks are generated by streamwise vortices associated to nonlinear features.

In particular, we study, for subcritical values of the Reynolds number, the response of the flow to a spatially localized forcing field oscillating with a given circular frequency ω. As a sample problem, we consider a localized pulsating disturbance immersed in the flow. This physical model is more suitable for the present analytical approach, because it allows for homogeneous boundary conditions. Afterward, we also consider the case of blowing and suction by reducing the nonhomogeneity of the boundary conditions to an equivalent forcing in the governing equations. As base flow, we consider a Poiseuille profile, $\underline{u}_0 = (1 - y^2, 0, 0)$, confined in the spatial region $\Omega = \{\underline{x} = (x, y, z) \in \mathbb{R}^3 | y \in (-1, 1)\}$. For this base flow, the critical Reynolds number is $\mathrm{Re}_C = 5772$ (see Orszag [13]). For small amplitudes, the oscillating forcing field drives a system of oblique waves. By increasing the amplitude, we observe new features of the flowfield that are characterized by streaky structures elongated in the streamwise direction. They are apparently generated by the interaction of oblique modes and become, for large time, a permanent aspect of the field.

We make here a perturbation expansion of the solution in terms of the amplitude of the disturbance ϵ (see Nayfeh [14] and Kevorkian and Cole [15]) truncated at second order [16]. The linearized solution, corresponding to the classical Orr–Sommerfeld, Squire system, is corrected at the second order to account for the quadratic interactions between first-order terms. When considering only the time asymptotic behavior, the streaks appear as a pseudoresonance of the system at second order, which may be explained in terms of the properties of non-normal operators.

In the following sections, we first describe the mathematical and the numerical model adopted, in sections 2 and 3, respectively. In section 4, we describe the physical mechanism that leads to the formation of the system of high- and low-speed streaks in the context of weakly nonlinear dynamics. The results of the perturbation analysis are discussed in section 5 by a comparison with corresponding DNS data. In section 6, we comment about the potential of the present approach to identify the most effective interactions to mimic the crucial physical events. Finally, in section 7, we describe the actual problem of blowing and suction at the boundary comparing the results to those of the pulsating disturbance immersed in the flow. Final comments and future applications are reported in section 8.

2. Mathematical model

In the following, the variables are made dimensionless with respect to half the height of the channel, the center line velocity of the base flow U_c, and the kinematic viscosity ν. The fluid flow is confined in the domain $\Omega = \{\underline{x} = (x, y, z) \in \mathbb{R}^3 | y \in (-1, 1)\}$ and its velocity is expressed in Cartesian components as

$$\underline{u}(\underline{x}, t) = u(\underline{x}, t)\underline{e}_1 + v(\underline{x}, t)\underline{e}_2 + w(\underline{x}, t)\underline{e}_3 = \underline{u}_\pi(\underline{x}, t) + v(\underline{x}, t)\underline{e}_2$$

where $\underline{u}_\pi(\underline{x}, t) = u(\underline{x}, t)\underline{e}_1 + w(\underline{x}, t)\underline{e}_3$ and $\underline{e}_i$, $i = 1, 2, 3$ is the canonical base of $\mathbb{R}^3$. Throughout the article, the subscript π denotes either the projection of a vector on the x–z plane or the suitable restriction of an operator to the x–z plane. Denoting with ∇ the gradient operator and adopting the standard notation for the Laplacian the motion of an incompressible fluid confined in Ω is described by the Navier–Stokes equations in the form

$$\begin{aligned} \frac{\partial \underline{u}_\pi}{\partial t} + \nabla_\pi p - \frac{1}{\mathrm{Re}}\Delta \underline{u}_\pi &= -N[\underline{u}, \underline{u}_\pi] + \underline{F}_\pi, \\ \frac{\partial v}{\partial t} + Dp - \frac{1}{\mathrm{Re}}\Delta v &= -N[\underline{u}, v] + F_y, \qquad \underline{x} \in \Omega, \qquad t > 0 \\ \nabla_\pi \cdot \underline{u}_\pi + Dv &= 0 \end{aligned} \tag{1}$$

where $p(\underline{x}, t)$ represents the dimensionless pressure field. The dot denotes the scalar product, $D = \partial/\partial y$ and $\mathrm{Re} = U_c h/\nu$ is the Reynolds number. For future convenience we have introduced the notation $N[a, b] = (\mathbf{a}\cdot\nabla)\mathbf{b}$, where $\mathbf{a}$ is a vector and $\mathbf{b}$ may be either a vector or a scalar, for the convective term to emphasize its structure as a bilinear operator. The vector

$$\underline{\mathbf{F}}(\underline{\mathbf{x}}, \mathbf{t}) = \mathbf{F_x}(\underline{\mathbf{x}}, \mathbf{t})\underline{\mathbf{e}}_\mathbf{1} + \mathbf{F_y}(\underline{\mathbf{x}}, \mathbf{t})\underline{\mathbf{e}}_\mathbf{2} + \mathbf{F_z}(\underline{\mathbf{x}}, \mathbf{t})\underline{\mathbf{e}}_\mathbf{3} = \underline{\mathbf{F}}_\pi + \mathbf{F_y}(\underline{\mathbf{x}}, \mathbf{t})\underline{\mathbf{e}}_\mathbf{2}$$

represents the external forces per unit mass.

We assume homogeneous boundary conditions

$$\underline{u}_\pi|_{y=\pm1} = \underline{0}, \qquad v|_{y=\pm1} = 0, \qquad (x, z) \in \mathbb{R}^2, t > 0 \tag{2}$$

and solenoidal initial conditions

$$\underline{u}_\pi(t=0) = \underline{u}_\pi^{(0)}, \qquad v(t=0) = v^{(0)}, \qquad \underline{x} \in \Omega. \tag{3}$$

where $\underline{u}_\pi^{(0)}$ and $v^{(0)}$ are two suitably given functions.

First of all, when $\underline{F}(\underline{x}, t) = \underline{0}$, and $\underline{u}_\pi^{(0)}(\underline{x}) = u_0(y)\underline{e}_1$, $v^{(0)}(\underline{x}) = 0$, with $u_0(y) = 1 - y^2$, the field

$$\underline{u}_0(\underline{x}, t) = u_0(y)\underline{e}_1, \qquad p_0(\underline{x}, t) = \left(\frac{\partial p}{\partial x}\right)_0 x + c, \qquad \underline{x} \in \Omega, t > 0 \tag{4}$$

where c is an arbitrary constant, and $(\partial p/\partial x)_0 = -2/\operatorname{Re}$, is the solution of (1), with the boundary and initial conditions (2), (3). The stationary solution (4) is the unperturbed solution or base flow.

We study the effect of a forcing term $\underline{F}(\underline{x}, t)$ on the unperturbed fluid motion (4) via perturbation theory by expanding the relevant variables in terms of the amplitude ϵ of the forcing,

$$q = q^{(0)} + \epsilon q^{(1)} + \epsilon^2 q^{(2)} + \epsilon^3 q^{(3)} + \cdots, \qquad \epsilon \to 0 \tag{5}$$

for $q = v, \underline{u}_\pi, p, \underline{F}$, where $\underline{u}_\pi^{(0)}, v^{(0)}, p^{(0)}$ are given by (4), and the remaining terms are unknowns to be determined by the perturbation analysis. We assume $\underline{F}^{(i)} = 0$, $i \neq 1$ and

$$F_y^{(1)} = \left(f_\omega(\underline{x})e^{j\omega t} + f_{-\omega}(\underline{x})e^{-j\omega t}\right), \qquad \underline{F}_\pi^{(1)} = 0 \tag{6}$$

where $\omega \in \mathbb{R}$ is the prescribed frequency, j is the imaginary unit, and $f_{\pm\omega}(\underline{x})$ are given functions to be specified later. Substituting (5) in (1), at order zero in ϵ the equations, and the corresponding boundary and initial conditions are satisfied by the base flow. At order 1 and 2, after recalling that $v^{(0)} = 0$ for the base flow (4), the equations become

$$\begin{aligned} \frac{\partial \underline{u}_\pi^{(1)}}{\partial t} + \nabla_\pi p^{(1)} - \frac{1}{\operatorname{Re}}\Delta \underline{u}_\pi^{(1)} + N[\underline{u}^{(0)}, \underline{u}_\pi^{(1)}] + N[\underline{u}^{(1)}, \underline{u}_\pi^{(0)}] &= 0 \\ \frac{\partial v^{(1)}}{\partial t} + Dp^{(1)} - \frac{1}{\operatorname{Re}}\Delta v^{(1)} + N[\underline{u}^{(0)}, v^{(1)}] &= F_y^{(1)} \\ \nabla_\pi \cdot \underline{u}_\pi^{(1)} + Dv^{(1)} &= 0, \end{aligned} \tag{7}$$

and

$$\begin{aligned} \frac{\partial \underline{u}_\pi^{(2)}}{\partial t} + \nabla_\pi p^{(2)} - \frac{1}{\operatorname{Re}}\Delta \underline{u}_\pi^{(2)} + N[\underline{u}^{(0)}, \underline{u}_\pi^{(2)}] + N[\underline{u}^{(2)}, \underline{u}_\pi^{(0)}] &= -N[\underline{u}^{(1)}, \underline{u}_\pi^{(1)}] \\ \frac{\partial v^{(2)}}{\partial t} + Dp^{(2)} - \frac{1}{Re}\Delta v^{(2)} + N[\underline{u}^{(0)}, v^{(2)}] &= -N[\underline{u}^{(1)}, v^{(1)}] \\ \nabla_\pi \cdot \underline{u}_\pi^{(2)} + Dv^{(2)} &= 0, \end{aligned} \tag{8}$$

respectively, with homogeneous boundary and initial conditions. The first-order equations (7) are driven by the external force term $\underline{F}^{(1)} = F_y^{(1)}\underline{e}_2$, while the second-order equations (8) are forced by the nonlinear interaction of the first-order terms $N[\underline{u}^{(1)}, \underline{u}^{(1)}] = N[\underline{u}^{(1)}, \underline{u}_\pi^{(1)}] + N[\underline{u}^{(1)}, v^{(1)}]\underline{e}_2$. For the chosen base flow, (7) and (8) are two linear systems whose coefficients depend only on the wall normal coordinate. By means of the usual manipulation used to derive the Orr–Sommerfeld, Squire equations both systems can be reduced to equivalent systems of equations for the normal component of the velocity $v^{(i)}$ and the normal component of the vorticity $\eta^{(i)} = \partial w^{(i)}/\partial x - \partial u^{(i)}/\partial z$, $i = 1, 2$. In this form, there is no explicit dependence on the pressure $p^{(i)}(\underline{x}, t)$, $i = 1, 2$. The two systems read

$$\frac{\partial}{\partial t} M\xi^{(i)} = L\xi^{(i)} + P\underline{T}^{(i)} \quad i = 1, 2 \tag{9}$$

where

$$\xi^{(i)} = \begin{pmatrix} v^{(i)} \\ \eta^{(i)} \end{pmatrix} \quad i = 1, 2$$

$$L = \begin{pmatrix} -u_0 \frac{\partial}{\partial x}\Delta + D^2 u_0 \frac{\partial}{\partial x} + \frac{1}{\mathrm{Re}}\Delta^2 & 0 \\ -Du_0 \frac{\partial}{\partial z} & -u_0 \frac{\partial}{\partial x} + \frac{1}{\mathrm{Re}}\Delta \end{pmatrix}$$

$$P = \begin{pmatrix} \Delta_\pi & -D\nabla_\pi \cdot \\ 0 & \underline{e}_2 \cdot \nabla_\pi \times \end{pmatrix} \quad M = \begin{pmatrix} \Delta & 0 \\ 0 & I \end{pmatrix}$$

$$\underline{T}^{(1)} = \begin{pmatrix} F_y^{(1)} \\ 0 \end{pmatrix} \quad \underline{T}^{(2)}(\underline{u}^{(1)}, \underline{u}^{(1)}) = \begin{pmatrix} -N\left[\underline{u}^{(1)}, v^{(1)}\right] \\ -N\left[\underline{u}^{(1)}, \underline{u}_\pi^{(1)}\right] \end{pmatrix}$$

with boundary conditions

$$v^{(i)} = Dv^{(i)} = \eta^{(i)} = 0 \tag{10}$$

at $y = \pm 1$ and initial conditions

$$\xi^{(i)}(t = 0) = 0, \qquad i = 1, 2. \tag{11}$$

Note that $\underline{T}^{(i)}$, $i = 1, 2$ is formally a vector with two components. The first corresponds to the wall normal component of the forcing, $F_y^{(i)}$. The second, itself a two-dimensional (2-D) vector, contains the projection of the forcing along the wall, $\underline{F}_\pi^{(i)}$. After system (9) is solved, the related velocity field is reconstructed by solving the equations

$$\nabla_\pi \cdot \underline{u}_\pi^{(i)} = -Dv^{(i)}$$
$$\underline{e}_2 \cdot \nabla_\pi \times \underline{u}_\pi^{(i)} = \eta^{(i)}, \quad i = 1, 2$$

corresponding to the conservation of mass and the definition of $\eta^{(i)}$, respectively. The solution of the system (9) can be split into two parts, the first one, $\xi^{(i)^L}$, properly describes the asymptotic evolution for long times, the second one, $\xi^{(i)^T}$, to be seen as a correction for short times, describes the initial transient behavior

$$\xi^{(i)} = \xi^{(i)^T} + \xi^{(i)^L}, \qquad i = 1, 2. \tag{12}$$

The form of the forcing term implies a solution at the first order

$$\xi^{(1)^L} = \xi_{\omega}^{(1)^L} e^{j\omega t} + \xi_{-\omega}^{(1)^L} e^{-j\omega t}$$

and equation (9) yields the three equations

$$(\pm j\omega M - L)\xi_{\pm\omega}^{(1)^L} = P\underline{T}_{\pm\omega}^{(1)} \tag{13}$$

$$\frac{\partial}{\partial t} M\xi^{(1)^T} = L\xi^{(1)^T} \quad \xi^{(1)^T}(t=0) = -\xi^{(1)^L}(t=0) \tag{14}$$

where $\underline{T}_{\pm\omega} = (f_{\pm\omega}, 0)^T$. Notice that the initial condition in eq. (14) is obtained from the decomposition (12), because the whole problem has zero initial conditions (11). Since M and L are linear operators, the solution of (14) can be written as a superposition of eigenmodes of $M^{-1}L$, which are known to form a complete base, see DiPrima, Habetler [17]

$$\xi^{(1)^T} = \sum_r a_r \bar{\xi}_r e^{\lambda_r t}$$

where $\bar{\xi}_r$ satisfies $M\lambda_r\bar{\xi}_r = L\bar{\xi}_r, \forall r \in \mathbb{Z}$ and $a_r, \forall z \in \mathbb{Z}$ are suitable coefficients to be determined. The related velocity field may be expressed as

$$\underline{u}^{(1)^T} = \sum_r \underline{u}_{\lambda_r}^{(1)^T} = \sum_r a_r \underline{u}_r^{(1)} e^{\lambda_r t}.$$

Concerning the long time behavior of the the solution at second order, the structure of the quadratic interaction term $\underline{T}^{(2)}(\underline{u}^{(1)^L}, \underline{u}^{(1)^L})$ implies

$$\xi^{(2)^L} = \xi_0^{(2)^L} + \xi_{2\omega}^{(2)^L} e^{j2\omega t} + \xi_{-2\omega}^{(2)^L} e^{-j2\omega t},$$

i.e., only the zero and 2ω frequency components are excited in the second order, time asymptotic solution. As in the previous case, the equations for the second order may be split into several equations,

$$-L\xi_0^{(2)^L} = P\underline{T}^{(2)}\left(\underline{u}_{\pm\omega}^{(1)^L}, \underline{u}_{\mp\omega}^{(1)^L}\right) \tag{15}$$

$$(\pm j2\omega M - L)\xi_{\pm 2\omega}^{(2)^L} = P\underline{T}^{(2)}\left(\underline{u}_{\pm\omega}^{(1)^L}, \underline{u}_{\pm\omega}^{(1)^L}\right)$$

$$\frac{\partial}{\partial t} M\xi^{(2)^T} = L\xi^{(2)^T} + P\underline{T}^{(2)}\left(\underline{u}_{\pm\omega}^{(1)^L}, \underline{u}_{\lambda_r}^{(1)^T}\right) + P\underline{T}^{(2)}\left(\underline{u}_{\lambda_r}^{(1)^T}, \underline{u}_{\pm\omega}^{(1)^L}\right) + P\underline{T}^{(2)}\left(\underline{u}_{\lambda_r}^{(1)^T}, \underline{u}_{\lambda_s}^{(1)^T}\right). \tag{16}$$

To simplify the notation, in equation (16) we have omitted the summation in r and s; i.e., we report only a representative term for each type of nonlinear forcing. The solution of (16) is expressed as the sum of a particular solution of the non homogeneous equation, $\xi_P^{(2)}$, and a solution of the corresponding homogeneous equation $\xi_H^{(2)}$,

$$\xi^{(2)^T} = \xi_H^{(2)} + \xi_P^{(2)} \tag{17}$$

where

$$\xi_P^{(2)} = \sum_r a_r \xi_{r,\omega}^{(2)} e^{(\lambda_r + j\omega)t} + \sum_r a_r \xi_{r,-\omega}^{(2)} e^{(\lambda_r - j\omega)t} + \sum_{r,s} a_r a_s \xi_{r,s}^{(2)} e^{(\lambda_r + \lambda_s)t}$$

and

$$[(\lambda_r \pm j\omega)M - L]\xi_{r,\pm\omega}^{(2)} = P\underline{T}^{(2)}\left(\underline{u}_{\pm\omega}^{(1)^L}, \underline{u}_{\lambda_r}^{(1)^T}\right) + P\underline{T}^{(2)}\left(\underline{u}_{\lambda_r}^{(1)^T}, \underline{u}_{\pm\omega}^{(1)^L}\right) \tag{18}$$

$$[(\lambda_r + \lambda_s)M - L]\xi_{r,s}^{(2)} = P\underline{T}^{(2)}\left(\underline{u}_{\lambda_r}^{(1)^T}, \underline{u}_{\lambda_s}^{(1)^T}\right) \tag{19}$$

$$\left(\frac{\partial}{\partial t}M - L\right)\xi_H^{(2)} = 0, \;\; \xi_H^{(2)}(t=0) = -\left(\xi^{(2)^L} + \xi_P^{(2)}\right)(t=0). \tag{20}$$

As in the linear case, the homogeneous solution can be written as a superposition of eigenmodes of $M^{-1}L$ as,

$$\xi_H^{(2)} = \sum_r b_r \bar{\xi}_r e^{\lambda_r t}$$

with suitable coefficients b_r. Note that in (15), (16) we have exploited the bilinear structure of $\underline{T}^{(2)}$.

3. Numerical method

Since the problem is described at each order by linear equations with coefficients which are constant with respect to x and z, we may consider their Fourier transform in the (x, z) plane. The resulting equations, which are the transformed version of (13), (14), (15), (18), (19), (20), can be reduced to one of the two following forms

$$(\mu\hat{M}_k + \hat{L}_k)\hat{x}_k^L = \hat{f}_k \tag{21}$$

$$\frac{\partial}{\partial t}\hat{M}_k\hat{x}_k^T = \hat{L}_k\hat{x}_k^T \quad \hat{x}_k(0) = \hat{x}_{0_k} \tag{22}$$

both with homogeneous boundary conditions. Here $k = (\alpha, \beta)$ represent the (2-D) wave vector corresponding to the physical coordinates x, z, $\hat{f}_k$ can be either a known forcing term (at order one) or a quadratic interaction term

(at order two). To apply a Galerkin formulation (see Canuto et al. [18]), we recast equations (21), (22) in a weak form to obtain,

$$\langle(\mu\hat{M}_k + \hat{L}_k)\hat{x}_k^L, \chi\rangle = \langle\hat{f}_k, \chi\rangle \qquad \forall\chi \tag{23}$$

$$\left\langle\frac{\partial}{\partial t}\hat{M}_k\hat{x}_k^T, \chi\right\rangle = \langle\hat{L}_k\hat{x}_k^T, \chi\rangle \qquad \forall\chi \tag{24}$$

where $\chi = (g, h)$ is a test function and

$$\langle\cdot,\cdot\rangle = \int_{-1}^{1} \cdot, \cdot\, dy.$$

Following the standard approach, we select a suitable set of basis functions which, truncated at $2N$ terms, reads

$$\chi_r = \begin{cases} (g_r, 0) & \text{for} \quad r = 1, \ldots, N \\ (0, h_{r-\mathrm{N}}) & \text{for} \quad r = N+1, \ldots, 2N. \end{cases}$$

Specifically, g_r and h_r are chosen as Legendre polynomials, ℓ_r, with a proper prefactor to enforce the boundary conditions, $g_r = Dg_r = h_r = 0$ at $y = \pm 1$, consistent with the boundary conditions (10)

$$g_r = (1-y^2)^2\ell_r \qquad h_r = (1-y^2)\ell_r,$$

see Spalart et al. [19] for a similar discretization procedure for the wall normal direction in the context of DNS of boundary layer flows. The expansion of $\hat{x}_k^L$ in terms of the selected basis reads as $\hat{x}_k^L = \sum_{r=1}^{2N}\hat{a}_r\chi_r$, and the Galerkin formulation for (23), after integration by parts with the given boundary conditions, yields the algebraic system

$$(\mu\tilde{M}_{rs} + \tilde{L}_{rs})\hat{a}_s = \langle\hat{f}_k, \chi_r\rangle \qquad r = 1, \ldots, 2N$$

where

$$\tilde{M}_{rs} = \begin{pmatrix} F_{rs} & 0 \\ 0 & E_{rs} \end{pmatrix} \tilde{L}_{rs} = \begin{pmatrix} G_{rs} & 0 \\ C_{rs} & H_{rs} \end{pmatrix}$$

$$F_{rs} = -\int_{-1}^{1} Dg_r\, Dg_s\, dy - |k|^2\int_{-1}^{1} g_r\, g_s\, dy \quad r, s = 1, \ldots, N$$

$$E_{rs} = \int_{-1}^{1} h_{r-N}\, h_{s-N}\, dy \quad r, s = N+1, \ldots, 2N$$

$$G_{rs} = j\alpha\int_{-1}^{1} u_0\, D^2g_r\, g_s\, dy - j\alpha|k|^2\int_{-1}^{1} u_0\, g_r\, g_s\, dy +$$

$$j\alpha\int_{-1}^{1} Du_0(Dg_r\, g_s + g_r\, Dg_s)dy - 1/\,\mathrm{Re}\int_{-1}^{1} D^2g_r\, D^2g_s\, dy$$

$$-2|k|^2/\,\mathrm{Re}\int_{-1}^{1} Dg_r\,Dg_s\,dy - |k|^4/\,\mathrm{Re}\int_{-1}^{1} g_r\,g_s\,dy \quad r,s=1,\ldots,N$$

$$C_{rs} = j\beta\int_{-1}^{1} Du_0\,g_r\,h_{s-N}\,dy \quad r=1,\ldots,N,\ s=N+1,\ldots,2N$$

$$H_{rs} = j\alpha\int_{-1}^{1} u_0\,h_{r-N}\,h_{s-N}\,dy + 1/\,\mathrm{Re}\int_{-1}^{1} Dh_{r-N}\,Dh_{s-N}\,dy + \frac{|k|^2}{\mathrm{Re}}\int_{-1}^{1} h_{r-N}\,h_{s-N}\,dy \quad r,s=N+1,\ldots,2N$$

with $|k|^2=\alpha^2+\beta^2$. The system is banded, with band width 13, and can be efficiently solved by proper inversion routines. In an analogous way, equation (24) is rewritten as

$$\tilde{M}_{rs}\frac{\partial}{\partial t}\hat{b}_s = \tilde{L}_{rs}\hat{b}_s.$$

The solution is then expressed as superposition of modes obtained as a solution of the generalized eigenvalue problem

$$\lambda^{(p)}\tilde{M}_{rs}\hat{\rho}_s^{(p)} = \tilde{L}_{rs}\hat{\rho}_s^{(p)} \quad p=1,\ldots,2N$$

where $\hat{\rho}^{(p)}$ is the p^{th} eigenvector and $\lambda^{(p)}$ is the corresponding eigenvalue. The solution is then given by

$$\hat{x}_k = \sum_{p=1}^{2N}\hat{b}_p\hat{\rho}^{(p)}e^{\lambda^{(p)}t}$$

where the coefficients $\hat{b}_p$ are determined by the initial conditions.

4. Nonlinear interactions as a generator of streamwise vorticity

The physical mechanism that induces the formation of a system of high- and low-speed streaks may be seen as a lift-up effect induced by vorticity structures originated by the nonlinear interactions. As a sample problem, we consider a spatially localized pulsating disturbance (6) in subcritical conditions. In particular, $f_{(\pm\omega)}(\underline{x})$ are chosen as Gaussian functions centered in x_0, y_0, z_0 of variance σ_x, σ_y, σ_z

$$f_{(\pm\omega)}(\underline{x}) = \frac{1}{\sqrt{8\pi^3}\sigma_x\sigma_y\sigma_z}e^{-\frac{(x-x_0)^2}{2\sigma_x{}^2}-\frac{(y-y_0)^2}{2\sigma_y{}^2}-\frac{(z-z_0)^2}{2\sigma_z{}^2}}$$

vibrating with a frequency ω. The specific values of the variance, see Figure 2, have been selected to ease the comparison with DNS results, see section 6.

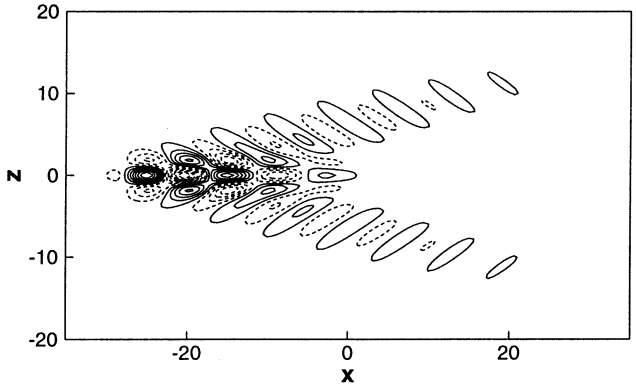

Figure 2. Linear case, streamwise perturbation velocity at $y = -0.75$. Re $= 3000$. The forcing term $f_{\pm\omega}$ is centered in $x_0 = -30.$, $y_0 = -.75$, $z_0 = 0$, with $\omega = .26$, $\sigma_x = 1.$, $\sigma_y = .1$, $\sigma_z = 1$. Only the significant part of the flow field is shown. Computational domain: $\Lambda_x = 120.$, $\Lambda_z = 60$.

We assume a bounded computational domain

$$\Omega_B = \{\underline{x} \in \mathbb{R}^3 | -\Lambda_x/2 < x < \Lambda_x/2, -1 < y < 1, -\Lambda_z < z < \Lambda_z\}$$

with periodical boundary conditions in x and z. Typically, in the results discussed hereafter we have considered $N_x = 65$, $N_z = 65$ harmonics in the two periodic directions. The wave numbers are given by

$$\alpha = n_x\alpha_0,\ \beta = n_z\beta_0, \qquad n_x = -N_x/2, \cdots, N_x/2, \quad n_z = -N_z/2, \cdots, N_z/2$$

where $\alpha_0 = 2\pi/\Lambda_x$, $\beta_0 = 2\pi/\Lambda_z$. In the wall-normal direction, the set of basis functions introduced in section 3 has been truncated at $2N = 80$ terms.

In the linear solution of the problem, this forcing generates a system of oblique waves that propagates in the streamwise direction, see Figure 2. For sufficiently small amplitude disturbances, the linear analysis is able to explain completely the physical evolution of the flow, because the nonlinear effects are negligible. For larger amplitudes, we expect that the nonlinear effects induce the generation of streamwise vorticity that is going to force, in turn, the lift-up phenomenon. This belief is supported by [9] where the nonlinear interactions of a pair of oblique waves creates streamwise-independent structures; i.e., streamwise vortices. The perturbation model of section 2 is able to capture this effect as an interaction between first-order terms. Actually, the interaction between modes associated to wave numbers $(\pm\alpha, \beta)$ forces the wave number $(0, 2\beta)$ and generates an elongated structure in the x-direction. The associated lift-up is shown in Figure 3: low momentum fluid is carried from the walls toward the center of the channel and vice versa by the effect of the streamwise vorticity to generate a low-speed streak. In Figure 4, we observe that the second-order contribution is strong enough to modify the

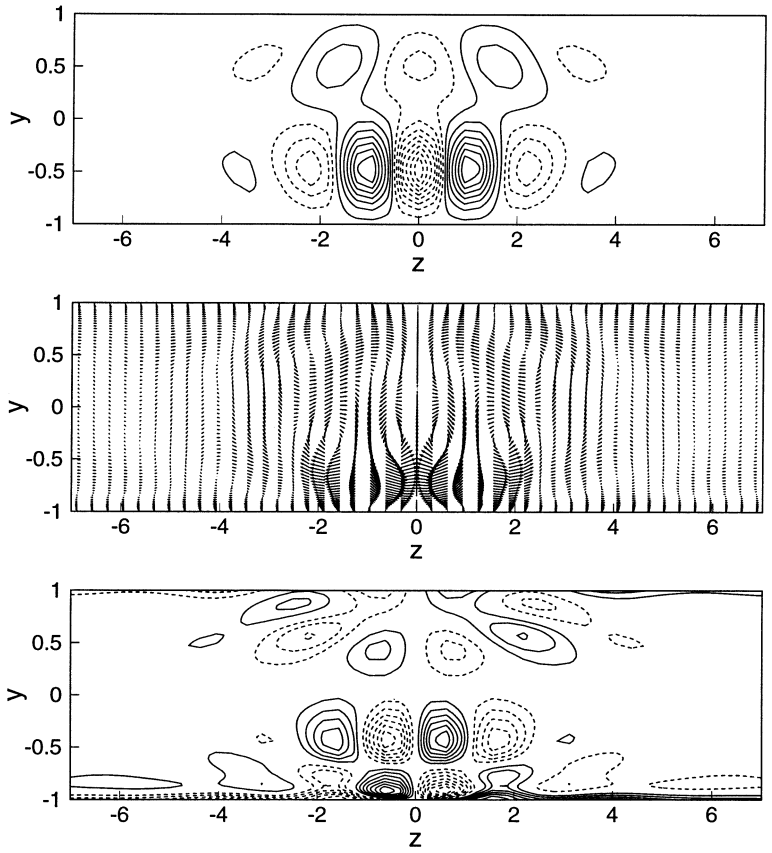

Figure 3. Lift-up effect $x = -30$. From the top to the bottom: streamwise perturbation velocity $u^{(2)}$ (negative dashed), vector field $(w^{(2)}, v^{(2)})$, and streamwise perturbation vorticity $\Omega_x^{(2)} = \partial w^{(2)}/\partial y - \partial v^{(2)}/\partial z$.

linear solution by giving raise to a low-speed streak. We stress here that a weakly nonlinear dynamics; i.e., second-order perturbation analysis, is able to isolate the dominant nonlinear features of the flow, thus providing a simple and efficient tool to analyze the basic mechanisms that are difficult to identify by an experimental or a direct numerical simulation.

5. Second-order terms: Perturbation solution versus DNS

To evaluate the capability of the perturbation method, we analyze here the previous results in comparison with DNS, see Henningson et al. [20] and references cited therein. In particular, we point out the features that we may capture with the present model at various orders. Clearly, we may expect, by

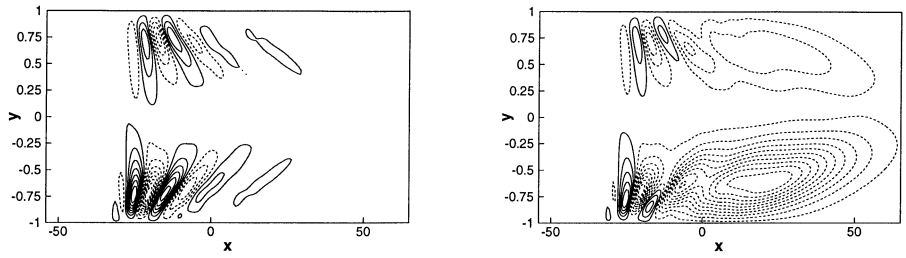

Figure 4. Weakly nonlinear approximation, streamwise perturbation velocity u at $x = -30$. Linear solution (left plot). Weakly nonlinear approximation (right plot). Amplitude of the external volume force $\epsilon = 0.5 \cdot 10^{-1}$.

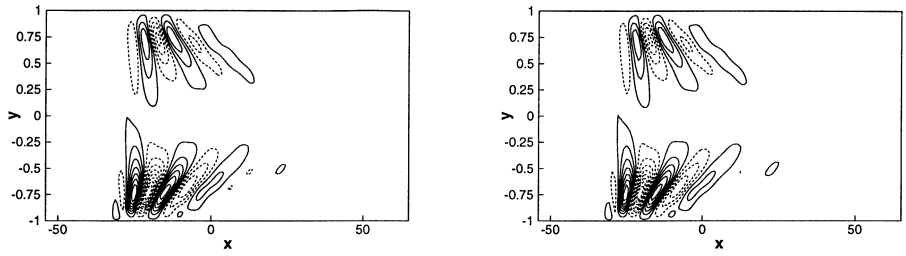

Figure 5. Linear approximation (left plot): contour lines of the streamwise velocity component $u^{(1)}$. DNS (right plot): contour lines of the streamwise velocity component u. $\epsilon = 0.5 \cdot 10^{-6}$. $t = 193$.

increasing the amplitude, to obtain only a qualitative agreement that is, however, completely lost for very large amplitudes. For small values of the amplitude of the disturbance, the solution of the linear Orr–Sommerfeld system of equation is in very good agreement with the solution of the Navier–Stokes equations, as shown in Figure 5 where the two solutions are compared. For the larger value of the amplitude; i.e., $\epsilon = 0.5 \cdot 10^{-1}$, new features arise, such as the system of low-speed streaks that seem as a steady feature of the flow in the limit as time goes to infinity. In fact, the linear analysis is not able to explain, in this case, the main aspects of the problem. In Figure 6 we compare the results of the second-order perturbation solution with those obtained by DNS. The elongated structures that emerge as the most significant new feature in DNS (right plot) are significantly well captured by the weakly nonlinear model, which accounts only for the effect of the interaction between first-order terms.

For a more quantitative evaluation of the present calculation we have analyzed the DNS result in terms of an amplitude expansion, isolating the linear, quadratic, and cubic part of the solution [20]. For small amplitude disturbance the DNS velocity field is expressed as

$$\underline{u}(\epsilon) = \epsilon \underline{u}^{(1)} + \epsilon^2 \underline{u}^{(2)} + \epsilon^3 \underline{u}^{(3)} + O(\epsilon^4), \ \epsilon \to 0. \tag{25}$$

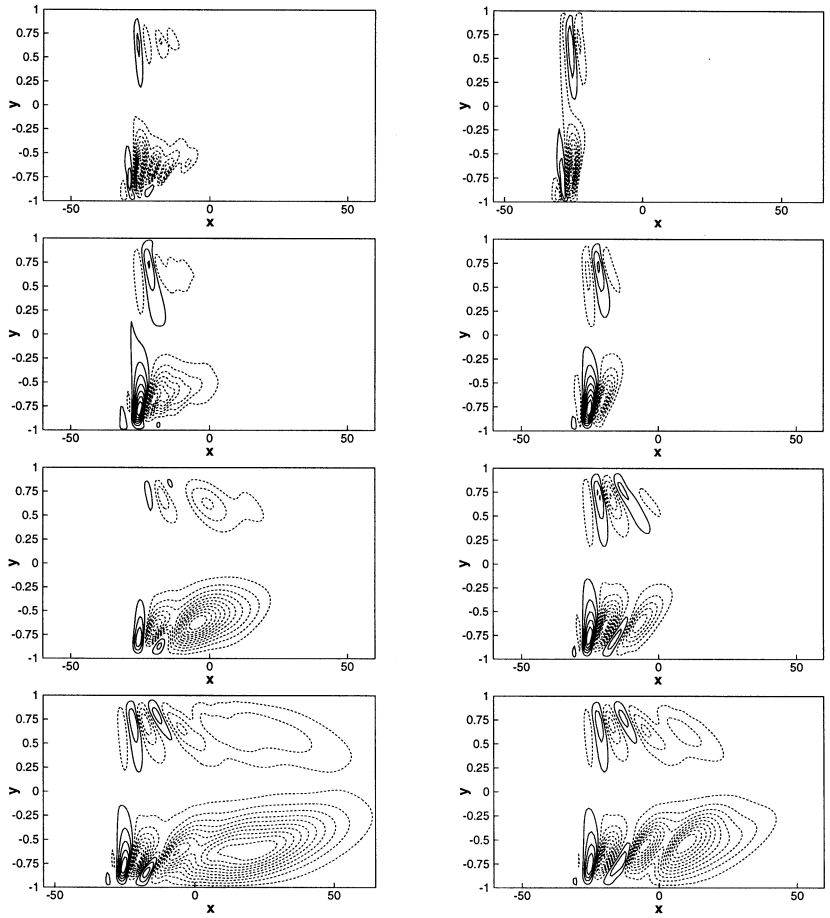

Figure 6. Weakly nonlinear approximation (left plot), DNS (right plot). Streamwise perturbation velocity on the symmetry plane $z = 30$. Time evolution $t = 12.08$, $t = 24.16$, $t = 48.33$, $t = 96.66$. $\epsilon = 0.5 \cdot 10^{-1}$.

We have evaluated $\underline{u}(\epsilon)$ for three different values of ϵ. Then, the three different contributions $\underline{u}^{(1)}, \underline{u}^{(2)}, \underline{u}^{(3)}$ can be calculated by enforcing (25) and solving the system

$$\begin{pmatrix} \epsilon_1 & \epsilon_1^2 & \epsilon_1^3 \\ \epsilon_2 & \epsilon_2^2 & \epsilon_2^3 \\ \epsilon_3 & \epsilon_3^2 & \epsilon_3^3 \end{pmatrix} \begin{pmatrix} \underline{u}^{(1)} \\ \underline{u}^{(2)} \\ \underline{u}^{(3)} \end{pmatrix} = \begin{pmatrix} \underline{u}(\epsilon_1) \\ \underline{u}(\epsilon_2) \\ \underline{u}(\epsilon_3) \end{pmatrix}.$$

Specifically, we have assumed $\epsilon_1 = 0.5 \cdot 10^{-6}$, $\epsilon_2 = 0.5 \cdot 10^{-5}$, and $\epsilon_3 = 0.5 \cdot 10^{-4}$. Figure 7 shows a comparison of the first- and the second-order corrections obtained from the weakly nonlinear model and from DNS coupled with the present technique. As expected, the agreement for the first order is very good

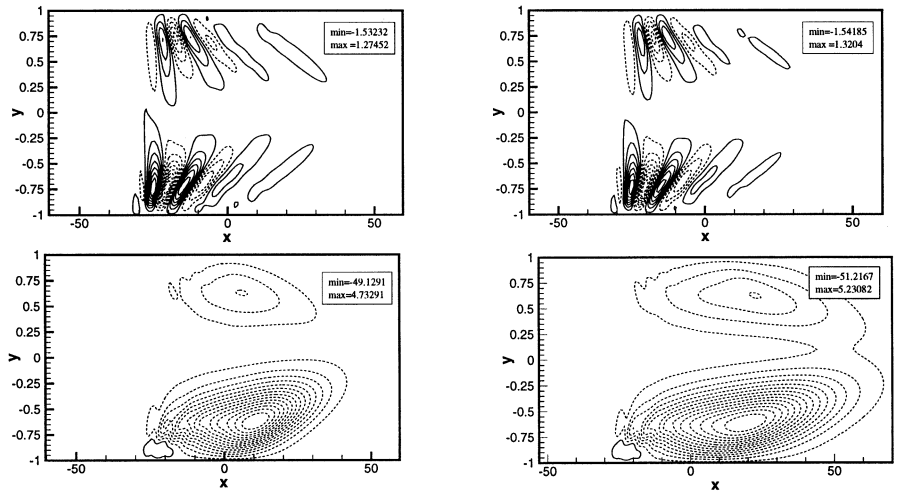

Figure 7. DNS: first- and second-order correction (left plot). Weakly nonlinear approximation: first- and second-order (right plot). Amplitude of the external volume force normalized to one. Contour lines of streamwise velocity component at $z = 30$.

and it is quite satisfactory also for the second-order correction where only small differences appear in Figure 7.

6. Selection of the most effective interactions

The perturbation analysis we have proposed to study transitional flows may offer a very suitable approach to determine the most effective nonlinear interactions that are going to govern the flow evolution. More specifically, by this procedure, any interaction among different modes may be isolated to evaluate its influence on the entire flowfield. In particular, if we focus our attention on the large time aspects of the flowfield, we can observe that among all the possible contributions, only those resulting in a zero frequency forcing, at second order, are responsible for the streaks formation. More precisely, in the limit as $t \to \infty$, the second-order correction has two contributions which present a completely different character. The first is associated with the frequency 2ω and represents a distortion of the linearized field, see Figure 8 (left plot), the other appears as a steady feature that is associated to zero frequency and corresponds to the streaky structure previously discussed, see Figure 7 (right plot). A quantitative analysis shows that the effect of the 2ω contribution is much lower than that associated to the zero frequency. All these observations may find a rational framework in terms of the pseudospectral analysis of the problem [5]. Actually the Orr–Sommerfeld, Squire operator is non-normal in the energy norm, and for such operators

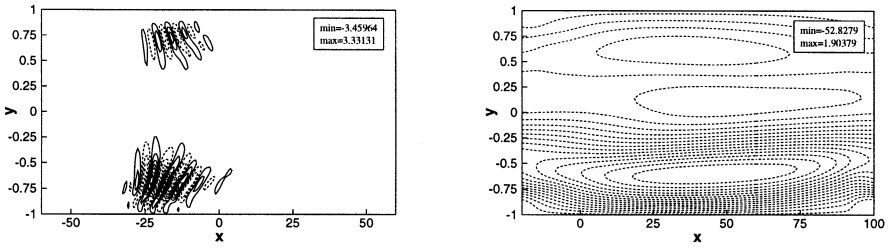

Figure 8. Weakly nonlinear approximation, $t \to \infty$. Contour lines of streamwise velocity component $u^{(2)^L}$ associated to a frequency 2ω (left plot) and to a zero frequency at $x = 30$. $\epsilon = 0.5 \cdot 10^{-4}$.

it is known that the analysis of the spectrum is insufficient to characterize the response to a given forcing field. Instead, the complete analysis of the norm of the resolvent should be performed leading to the concept of pseudospectra and pseudoresonance. When such analysis is performed for the present operator [5], the highest response for real frequency corresponds to a forcing field characterized by $\alpha = \omega = 0$. These mathematical properties largely explain the physical observations of section 4, which confirm the quadratic forcing terms as responsible for the appearance of streamwise vorticity, which in its turn originate the lift-up effect leading to the streak formation. To focus the selection process even more, we may retain, among all the possible nonlinear first-order interactions, only those responsible for the streaks formation; namely, only the interactions that force wave numbers with α approximately zero. Figure 9 represents the spectral amplitude of the forcing terms for the second-order equations, together with that of the linear solution. As expected, the forcing is concentrated in a region of the spectral space in a neighborhood of $\alpha = 0$, with β approximately two times the value associated to the maximum of the spectrum of the linear solution. By selecting the interactions according to this procedure, we are able to select the essential interactions to isolate the process of streaks formation from the background field.

7. Application to blowing and suction

In the previous sections, we have introduced a weakly nonlinear model able to capture some important nonlinear features of the flow in the case of homogeneous boundary conditions. We have considered a spatially localized disturbance harmonic in time, which should be seen as a prototype model for a blowing or suction at the walls. Here, we analyze directly the effect of blowing or suction at one of the two walls, which, hereafter, we refer to as the disturbance wall. This problem is considered of relevance for possible control devices aimed at retarding or avoiding transition and has been investigated

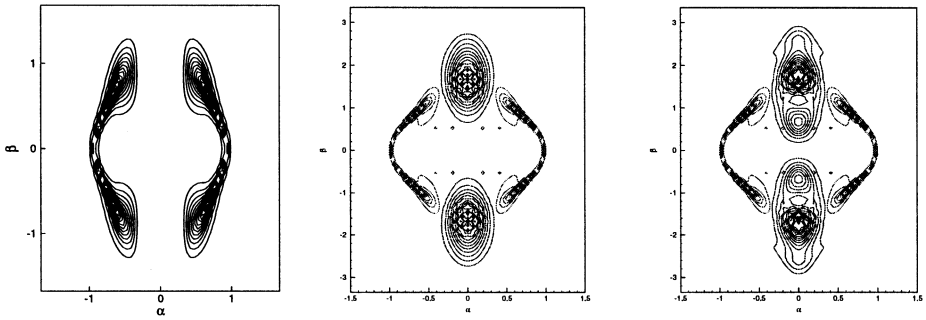

Figure 9. Spectral amplitude: linear solution (left plot), linear solution and second-order forcing term, Orr–Sommerfeld (central plot), Squire (right plot).

either experimentally or by DNS (see Koslov and Ramazanov [21], Gaster and Grant [22], [23]). For nonhomogeneous data at the wall, the problem can be transformed in an equivalent one where the originally nonhomogeneous boundary conditions result in a known forcing term for the equations. In the following, we assume $\underline{F}(\underline{x}, t) = \underline{0}$, see equation (6), and boundary conditions for the disturbance wall

$$\underline{u}_{\pi}^{(1)}|_{y=-1} = 0 \tag{26}$$

$$v^{(1)}|_{y=-1} = \frac{1}{2\pi\sigma_x\sigma_z} e^{-\frac{(x-x_0)^2}{2\sigma_x^2}} e^{-\frac{(z-z_0)^2}{2\sigma_z^2}} e^{j\omega t} = v_-. \tag{27}$$

At the other wall, to enforce the conservation of mass, we apply

$$\underline{u}_{\pi}^{(1)}|_{y=1} = 0 \tag{28}$$

$$v^{(1)}|_{y=1} = \frac{1}{\Lambda_x\Lambda_x} e^{j\omega t} = v_+, \tag{29}$$

where Λ_x, Λ_z are the dimensions of the numerical domain. The solution at first order may be written as a superposition of two terms

$$\underline{u}^{(1)} = \bar{\underline{u}}^{(1)} + \tilde{\underline{u}}^{(1)} \tag{30}$$

where $\tilde{\underline{u}}^{(1)}$ is a solenoidal field which is requested to satisfy the boundary conditions of the original problem

$$\tilde{\underline{u}}_{\pi}^{(1)}|_{\pm 1} = 0, \quad \tilde{v}^{(1)}|_{y=-1} = v_-, \quad \tilde{v}^{(1)}|_{y=1} = v_+.$$

The other, $\bar{\underline{u}}^{(1)}$, is a vector field with homogeneous boundary conditions,

$$\bar{\underline{u}}_{\pi}^{(1)}|_{y=\pm 1} = 0, \quad \bar{v}^{(1)}|\pm 1 = 0,$$

satisfying the equations (7) with forcing term $\underline{F}_\pi$, F_y given as

$$\underline{F}_\pi = -\left[\frac{\partial \tilde{\underline{u}}_\pi^{(1)}}{\partial t} + N[\underline{u}^{(0)}, \tilde{\underline{u}}_\pi^{(1)}] + N[\tilde{\underline{u}}^{(1)}, \underline{u}_\pi^{(0)}] - \frac{1}{\mathrm{Re}}\Delta \tilde{\underline{u}}_\pi^{(1)}\right]$$

$$F_v = -\left[\frac{\partial \tilde{v}^{(1)}}{\partial t} + N[\underline{u}^{(0)}, \tilde{v}^{(1)}] - \frac{1}{\mathrm{Re}}\Delta \tilde{v}^{(1)}\right].$$

Hence $\underline{u}^{(1)}$, given by (30) is a solution of the original problem with non-homogeneous boundary conditions. Following the technique introduced in section 2, we obtain at first order a system of equations in $\bar{\xi}^{(1)} = (\bar{v}^{(1)}, \bar{\eta}^{(1)})^T$ satisfying homogeneous boundary conditions, which is forced by a known forcing term

$$\frac{\partial}{\partial t} M \bar{\xi}^{(1)} - L\bar{\xi}^{(1)} = -\frac{\partial}{\partial t} M \tilde{\xi}^{(1)} + L\tilde{\xi}^{(1)}, \tag{31}$$

where $\tilde{\xi}^{(1)} = (\tilde{v}^{(1)}, \tilde{\eta}^{(1)})$. Concerning the second-order correction, because the corresponding boundary conditions are homogeneous, the procedure is the same as previously discussed in section 4. In this way, the effect of the blowing and suction at the disturbance wall results, at the second order, in the generation of streamwise vorticity that induces the formation of a system of high- and low-speed streaks. The numerical results we obtain for this case may be analyzed and compared with those discussed before for the vibrating button. Figure 10 shows the results for the two kinds of disturbance.

From the top to the bottom, we have represented the first-order solution, the second-order correction, and, finally, the superposition of the two, for the blowing and suction (left plot) and for the vibrating button (right plot). We observe from a qualitative point of view a very good agreement between the two cases, which lets us presume that the analysis presented for the vibrating button may be adapted, at least with regard to the main conclusions, to the blowing and suction disturbance.

8. Final comments and perspectives

The formation of the main structures of the flow induced by a localized disturbance has been observed by using a perturbation model, in terms of an amplitude expansion of the solution, truncated at the second order. The streamwise vorticity appears as a second-order effect in the flowfield because of the nonlinear interactions between the system of oblique waves. The generation of high- and low-speed streaks as a consequence of the lift-up associated with the presence of streamwise voritcity may be fully explained in the context of weakly nonlinear dynamics. To this end, we have evaluated the present results, comparing order by order, with the corresponding terms extracted

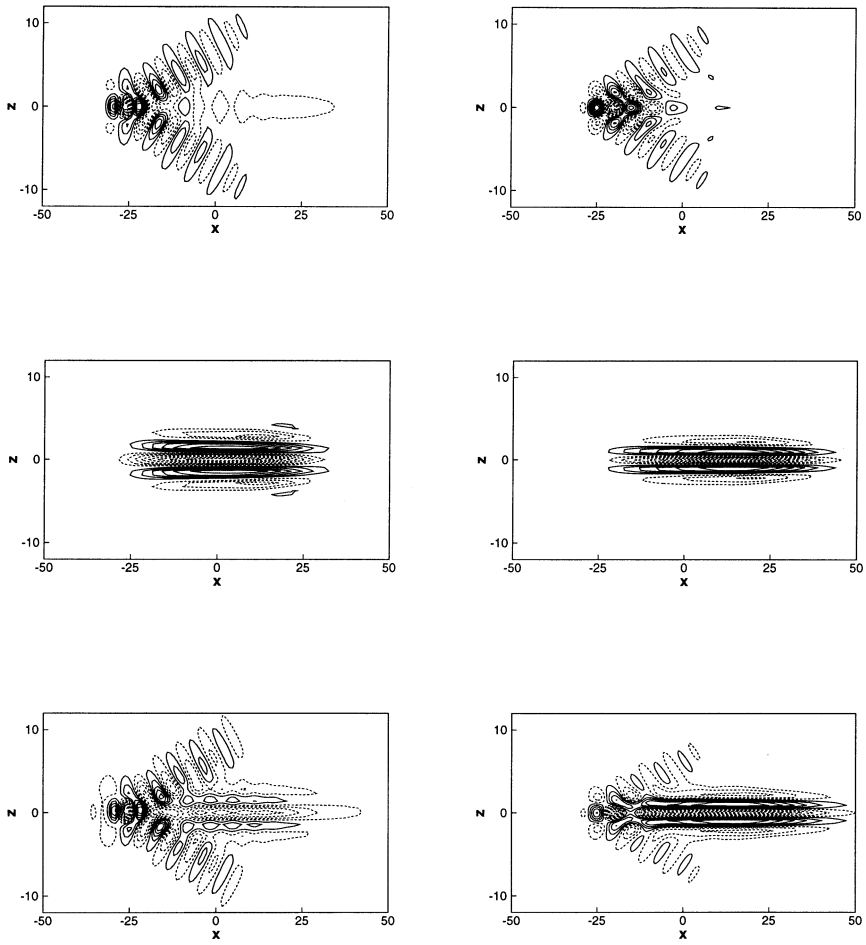

Figure 10. Streamwise component of velocity at first and second order. The bottom part gives the nonlinear solution as obtained by the perturbation method. Left: Blowing and suction at the wall. Right: Pulsating disturbance immersed in the flow.

from DNS data. We have shown that the proposed model is able to capture some of the essential nonlinear features of transitional flows, such as formation of streamwise vortices and systems of high- and low-speed streaks. We presently are using the same approach to understand more complex aspects of the dynamics of transition. In particular, because the sequence streamwise vortices–streaks formation–streaks instability–vortices regeneration is considered as fundamental in the early process of transition to turbulence, the aim is to select, by this procedure, the minimum number of modes able to mimic the basic sequence of events. As a final point, we comment on the possible extension of the present perturbation procedure to flows that are unbounded

in the wall-normal direction (e.g., boundary layers). In this case, the inversion of the linear operator involved at the different orders of the expansion could be performed, in principle, following the approach proposed by Criminale and Drazin [24] in the context of a linearized approach.

Acknowledgment

We would like to thank Professor D. Hennington for his interest in our work and for providing the DNS code for the comparisons. We are also grateful to Professor W. O. Criminale for the fruitful discussions while he was visiting the University of Roma.

References

1. P. G. Drazin and W. H. Reid, *Hydrodynamic Stability*, Cambridge University Press, Cambridge, UK, 1981.
2. J. T. Stuart, The production of intense shear layers by vortex stretching and convection, *Agard Rept.* 514:1–31 (1965).
3. T. Ellingsen and E. Palm, Stability of linear flow, *Phys. Fluids* 18:487 (1975).
4. M. T. Landhal, A note on an algebraic instability of inviscid parallel shear flows, *J. Fluid Mech.* 98:243 (1980).
5. L. N. Trefethen, A. E. Trefethen, S. C. Reddy, and T. A. Driscol, Hydrodynamic stability without eigenvalues, *Science* 261:578–584 (1993).
6. S. C. Reddy, P. J. Schmid, and D. S. Henningson, Pseudospectra of the Orr–Sommerfeld operator, *SIAM J. Appl. Math.* 53:15–47 (1993).
7. K. M. Butler and B. F. Farrel, Three-dimensional optimal perturbations in viscous shear flows, *Phys. Fluids A* 4(8):1637–1650 (1992).
8. S. Reddy, P. Schmid, J. S. Baggett, and D. Henningson, On the stability of streamwise streaks and transition thresholds in plane channel flows, *J. Fluid. Mech.* 365:269–303 (1998).
9. P. J. Schmid and D. S. Henningson, A new mechanism for rapid transiiton involving a pair of oblique waves, *Phys. Fluids A* 4(9):1986–1989 (1992).
10. D. S. Henningson and P. J. Schimd, Vector eigenfunction expansions for plane channel flows, *Stud. Appl. Math.* 87:15–43 (1992).
11. M. Gaster, A theoretical model of a wave packet in the boundary layer on a flat plate, *Proc. R. Soc. Lond.* 347:271–289 (1975).
12. W. O. Criminale, T. L. Jackson, D. G. Lasseigne, and R. D. Joslin, Perturbation dynamics in viscous channel flows, *J. Fluid. Mech.* 339:55–75 (1997).
13. S. A. Orszag, Accurate solution of the Orr–Sommerfeld stability equation, *J. Fluid Mech.* 50:689 (1971).
14. A. Nayfeh, *Perturbation Methods*, John Wiley and Sons, Inc., New York, 1973.
15. J. Kevorkian and J. D. Cole, *Perturbation Methods in Applied Mathematics*, Springer, New York, 1985.

16. D. Ponziani, C. M. Casciola, and F. Zirilli, Nonlinear effects and transition to turbulence in a wall-bounded flow, IV Congresso Nazionale SIMAI98, Giardinin Naxos, 1998.

17. R. C. Diprima and G. J. Habetler, A completeness theorem for nonselfadjoint eigenvalue problems in hydrodynamic stability, *Arch. Rat. Mech. Anal.* 32:218–227 (1969).

18. C. Canuto, M. H. Hussiani, A. Quarteroni, and T. A. Zang, *Spectral Methods in Fluid Dynamics*, Springer-Verlag, Berlin, 1987.

19. P. R. Spalart, R. D. Moser, and M. M. Rogers, Spectral methods for the Navier–Stokes equations with one infinite and two periodic directions, *J. Comp. Phys.* 96:297–324 (1991).

20. D. S. Henningson, A. Lundbladh, and A. V. Johansson, A mechanism for bypass transition from localized disturbances in wall-bounded shear flows, *J. Fluid Mech.* 250:169–207 (1993).

21. V. V. Koslov, and M. P. Ramazanov, Development of finite-amplitude disturbances in Poiseuille flow, *J. Fluid Mech.* 147:149–157 (1984).

22. M. Gaster and I. Grant, An experimental investigation of the formation and development of a wave packet in a laminar boundary layer, *Proc. R. Soc. Lond.* 347:253–269 (1975).

23. C. M. Casciola, A. Olivieri, and R. Piva, Transient response to harmonic excitations in Poiseuille flows, Third European Fluid Mechanics Conferences, Gottingen, 1997.

24. W. O. Criminale, and P. G. Drazin, The evolution of linearized perturbations of parallel flows, *Stud. Appl. Math.* 83:123–157 (1990).

Universitá di Roma

(Received May 26, 1999)